J. Plasma Physics (2009), *vol.* 75, *part* 1, *pp.* 19–33.
doi:10.1017/S0022377807007015 Printed in the United Kingdom

A comparative study of the filamentation and Weibel instabilities and their cumulative effect. I. Non-relativistic theory

M. LAZAR[1,2], A. SMOLYAKOV[1], R. SCHLICKEISER[2] and P. K. SHUKLA[2]

[1] Department of Physics and Engineering Physics, University of Saskatchewan, 116 Science Place, Saskatoon, Saskatchewan S7N 5E2, Canada

[2] Institut für Theoretische Physik, Lehrstuhl IV: Weltraum- und Astrophysik, Ruhr-Universität Bochum, D-44780 Bochum, Germany
(ps@tp4.ruhr-uni-bochum.de)

(Received 30 October 2007 and in revised form 6 November 2007, first published online 25 January 2008)

Abstract. A comparative study of the electromagnetic instabilities in anisotropic unmagnetized plasmas is undertaken. The instabilities considered are the filamentation and Weibel instability, and their cumulative effect. Dispersion relations are derived and the growth rates are plotted systematically for the representative cases of non-relativistic counterstreaming plasmas with isotropic or anisotropic velocity distributions functions of Maxwellian type. The pure filamentation mode is attenuated by including an isotropic Maxwellian distribution function. Moreover, it is observed that counterstreaming plasmas can be fully stabilized by including bi-Maxellian distributions with a negative thermal anisotropy. This effect is relevant for fusion plasma experiments. Otherwise, for plasma streams with a positive anisotropy the filamentation and Weibel instabilities cumulate leading to a growth rate by orders of magnitude larger than that of a simple filamentation mode. This is noticeable for the quasistatic magnetic field generated in astrophysical sources, and which is expected to saturate at higher values and explain the non-thermal emission observed.

1. Introduction

Electromagnetic instabilities of Weibel type are non-resonant and arise in plasmas with thermal anisotropies [1], or in those dominated by electrical streams [2]. Such systems are unstable to any harmonic perturbation and provide electromagnetic modes growing exponentially in time but not propagating. These instabilities can therefore explain the existence of strong quasistatic magnetic fields [3–5] or the acceleration of plasma particles [6] in many astrophysical sources where the non-thermal radiation originates. Moreover, the aperiodic instabilities are presently investigated in order to reduce the perturbations in the fast ignition scenario (FIS) for inertial confinement fusion [7–11].

Weibel [1] originally described the anisotropic temperature instability which propagates into a bi-Maxwellian plasma along the lower temperature axis, $T_\perp > T_\parallel$ and $\mathbf{k} = \mathbf{k}_\parallel$ (Sec. 3.2). Fried [2], trying to explain the physical mechanism responsible for the Weibel instability, has in fact described the counterstreaming-based instability propagating along the perpendicular direction with respect to the

streams, $\mathbf{k} \perp \mathbf{v}_0$, and which today is called the filamentation instability (Sec. 3.1). Despite their common origin into the bi-axis anisotropy of velocity distribution function, these two instabilities are markedly different. Filamentation instability, for example, develops even within a cold counterstreaming plasma, as shown in Sec. 3.1.1, whereas Weibel instability arises in thermally anisotropic plasmas with distributions of Maxwellian [12–15] or non-Maxwellian type [16–18].

A frequent confusion between Weibel and filamentation instabilities is observed, while the first remarks on their clear distinction can be noticed within the first works on the stabilization of beam–plasma systems [19–23]. Owing to their relevant consequences for both astrophysical and laboratory applications, there is, presently, a strong interest to show how both instabilities can exist independently, or interact to yield larger or lower growth rates [11, 24]. In the former case the quasistatic magnetic fields turns out to saturate at higher values expected to explain the synchrotron radiation detected from many astrophysical sources [3–5], whereas the reduction of filamentation instability is imperative for the FIS settings [7, 8, 11].

Tautz and Schlickeiser have derived the general dispersion relations in counterstreaming Maxwellian plasmas of arbitrary composition for longitudinal and transverse modes propagating parallel [25, 26] or perpendicular [27] to the streaming direction. Moreover, magnetic field amplification has been reported recently in numerical experiments for the filamentation instability in magnetized counterstreaming electron–positron plasmas with anisotropic temperatures [28]. In the present work, we rather choose to investigate purely growing filamentation modes with wave-vector normal to the plasma streams, and demonstrate that they are very sensitive to the plasma thermal anisotropy degree owing to their linear coupling with Weibel modes.

In this series of papers we intend to show how important the cumulative effect of Weibel and filamentation instabilities can be, providing numerical estimations for their growth rates. In order to perform a comparative study we plot systematically the growth rates of purely growing electromagnetic modes for different configurations: counterstreaming plasmas with isotropic (Secs 3.1.2 and 3.1.3) or anisotropic (Sec. 4) thermal distributions. The plasma system is taken to be homogeneous, charge and current neutralized, and in this first paper, we limit to a non-relativistic treatment assuming sufficiently small values for streaming and thermal velocities.

2. Basic framework

In order to investigate the linear wave modes developed in a collisionless plasma system without any stationary fields ($\mathbf{E}_0 = 0$ and $\mathbf{B}_0 = 0$), we follow the standard formalism of kinetic theory using the linearized Vlasov equation [12]

$$\frac{\partial f_a}{\partial t} + \mathbf{v} \cdot \frac{\partial f_a}{\partial \mathbf{r}} = -q_a \left[\mathbf{E} + \frac{\mathbf{p} \times \mathbf{B}}{m_a \gamma c} \right] \cdot \frac{\partial f_{a0}}{\partial \mathbf{p}}, \tag{1}$$

where $f_a(\mathbf{r}, \mathbf{p}, t)$ is the first-order perturbation of the equilibrium distribution function $f_{a0}(\mathbf{p})$ of the particles of type a, and normalized by

$$\int d\mathbf{p}\, f_{a0}(\mathbf{p}) = 1. \tag{2}$$

The anisotropic character of $f_{a0}(\mathbf{p})$ translates into

$$\frac{\partial f_{a0}}{\partial \mathbf{p}} \nparallel \mathbf{p} \tag{3}$$

https://doi.org/10.1017/S0022377807007015 Published online by Cambridge University Press

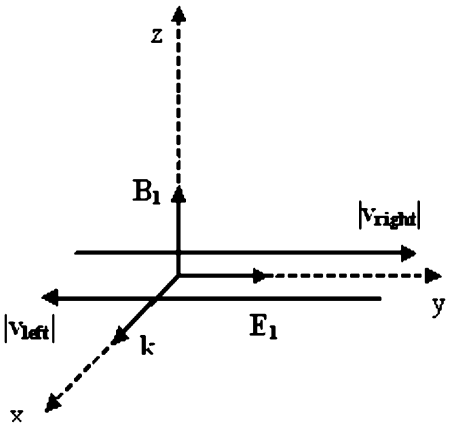

Figure 1. Two shells of counterstreaming plasmas and filamentation mode with fields $\mathbf{E}_1$, $\mathbf{B}_1$ and wave vector $\mathbf{k}$.

implying that

$$(\mathbf{p} \times \mathbf{B}) \cdot \frac{\partial f_{a0}}{\partial \mathbf{p}} \neq 0, \tag{4}$$

which is responsible for the linear unstable solution [13].

The conductivity tensor, σ, is given by the Ohm's law

$$\mathbf{J} = \sigma \cdot \mathbf{E} = \sum_a q_a \int_{-\infty}^{\infty} d\mathbf{p}\, \mathbf{v} f_a(\mathbf{r}, \mathbf{p}, t), \tag{5}$$

where the linear perturbation, f_a, is solution of (1) and using Maxwell equations, it is finally derived as follows

$$f_a = -\frac{\imath q_a}{\omega}\left(\mathbf{E} + \frac{\mathbf{p} \cdot \mathbf{E}}{m_a \gamma \omega - \mathbf{k} \cdot \mathbf{p}}\mathbf{k}\right) \cdot \frac{\partial f_{a0}}{\partial \mathbf{p}}. \tag{6}$$

The dielectric tensor is defined by $\epsilon_{ij} = \delta_{ij} + (4\pi\imath/\omega)\sigma_{ij}$, and with σ from (5) and (6), we obtain the dispersion relation for the linear unstable transverse modes

$$\frac{k^2 c^2}{\omega^2}\delta_{ij} = \epsilon_{ij} = \delta_{ij} + \sum_a \frac{\omega_{\mathrm{p},a}^2}{\omega^2}\left[\int_{-\infty}^{+\infty} d\mathbf{p}\, \frac{p_i}{\gamma}\frac{\partial f_{a,0}}{\partial p_j} + \int_{-\infty}^{+\infty} d\mathbf{p} \frac{1}{m_a \gamma \omega - \mathbf{k} \cdot \mathbf{p}}\left(\mathbf{k} \cdot \frac{\partial f_{a,0}}{\partial \mathbf{p}}\right)\frac{p_i p_j}{\gamma}\right]. \tag{7}$$

3. Filamentation instability versus Weibel instability: non-relativistic theory

3.1. Pure filamentation instability

The filamentation instability is the electromagnetic unstable mode, developed non-resonantly, i.e. $\Re(\omega) = \omega_{\mathrm{r}} = 0$, in a counterstreaming structure of plasmas, or in a beam–plasma system where the electron beam passing through the plasma quickly creates a return current. Such a counterstreaming configuration is presented schematically in Fig. 1, where the filamentation instability is emitted perpendicular to

https://doi.org/10.1017/S0022377807007015 Published online by Cambridge University Press

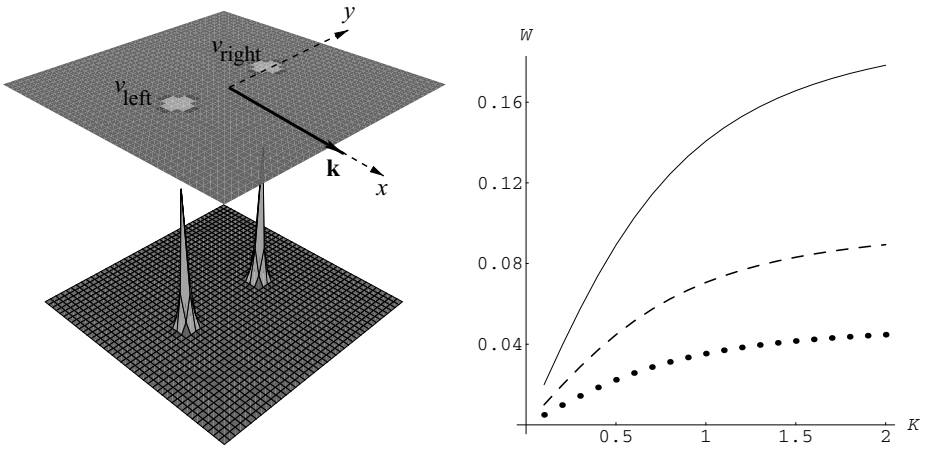

(a) (b)

Figure 2. (a) Distribution function for two cold counterstreaming plasmas represented in (8). (b) Growth rates of the filamentation instability obtained as solutions of (9), and corresponding to three non-relativistic values of the streaming velocity, $v_0/c = 0.05$ (dotted curve), $v_0/c = 0.1$ (dashed curve) and $v_0/c = 0.2$ (solid curve).

the streaming direction and has the electric field along the streaming direction. For the sake of simplicity, the two counterstreams are assumed to be symmetric with $v_\mathrm{l} = v_\mathrm{r} = v_0$, and with equal intensities, everywhere throughout our work.

3.1.1. Monochromatic (cold) counterstreaming plasmas. We first consider the simplest case of two cold counterstreaming plasmas, described by Fried [2] with the following distribution function:

$$f_0(v_x, v_y, v_z) = \delta(v_x)\delta(v_y^2 - v_0^2)\delta(v_z) = \tfrac{1}{2}\delta(v_x)[\delta(v_y - v_0) + \delta(v_y + v_0)]\delta(v_z), \quad (8)$$

which is presented schematically in Fig. 2(a). Substituting (8) in (7) leads to dispersion relation for the transverse unstable modes propagating along x-axis (perpendicular to the streaming direction) [2]

$$\epsilon_{yy} = 1 - \frac{\omega_\mathrm{pe}^2}{\omega^2}\left(1 + \frac{k^2 v_0^2}{\omega^2}\right). \quad (9)$$

The role of ions is minimized to that of a neutralizing background and the aperiodic solutions of (9), $\omega_\mathrm{r} = 0$ and $\Im(\omega) = \omega_\mathrm{i} > 0$, correspond to the filamentation instability, and are plotted in Fig. 2(b). We use the normalized quantities $W = \omega_\mathrm{i}/\omega_\mathrm{pe}$ and $K = kc/\omega_\mathrm{pe}$.

3.1.2. Asymmetric cold/thermal counterstreaming plasmas. Two asymmetric counterstreams are considered now, one stream of a cold plasma and the second stream of a thermal plasma with a Maxwellian distribution, so that they are described by the following distribution function:

$$f_0(v_x, v_y, v_z) = \frac{1}{2}\left[\frac{1}{\pi^{3/2} v_\mathrm{th}^3}\exp\left(-\frac{v_x^2 + (v_y + v_0)^2 + v_z^2}{v_\mathrm{th}^2}\right) + \delta(v_x)\delta(v_y - v_0)\delta(v_z)\right], \quad (10)$$

https://doi.org/10.1017/S0022377807007015 Published online by Cambridge University Press

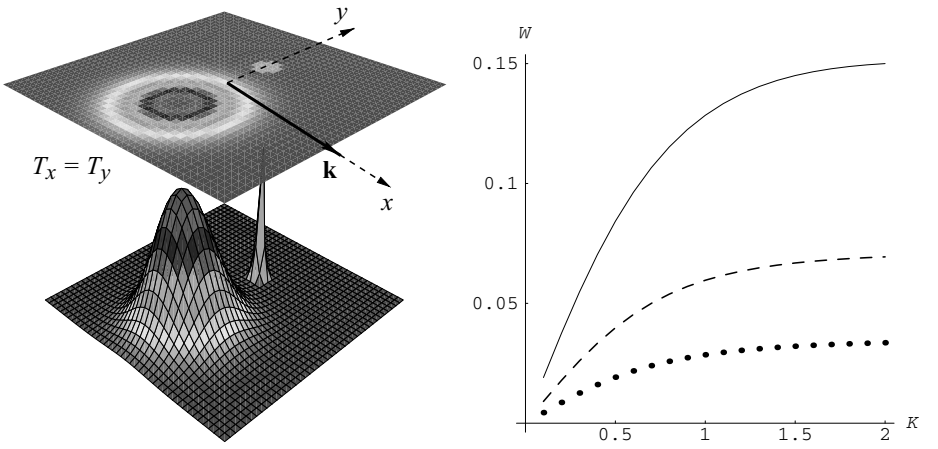

(a) (b)

Figure 3. (a) Distribution function for two asymmetric counterstreams plasmas represented in (10). (b) Growth rates of the filamentation instability obtained as solutions of (11), with $v_{\rm th}/c = 0.1$ and for the same values of the streaming velocity, $v_0/c = 0.05$ (dotted curve), $v_0/c = 0.1$ (dashed curve) and $v_0/c = 0.2$ (solid curve).

which is shown in Fig. 3(a). Using (10) in (7) we find the dielectric constant

$$\epsilon_{yy} = 1 - \frac{\omega_{\rm pe}^2}{2\omega^2}\left(1 + \frac{k^2 v_0^2}{\omega^2}\right) - \frac{\omega_{\rm pe}^2}{2\omega^2}\left[1 + \frac{1}{2}\left(1 + \frac{2v_0^2}{v_{\rm th}^2}\right) Z'\left(\frac{\omega}{k v_{\rm th}}\right)\right], \qquad (11)$$

in terms of the well-known plasma dispersion function [29]

$$Z(f) = \pi^{-1/2} \int_{-\infty}^{\infty} dx \, \frac{\exp(-x^2)}{x - f}, \quad f = \frac{\omega}{k v_{\rm th}}. \qquad (12)$$

The aperiodic solutions of (11) are plotted in Fig. 3(b). Owing to the finite temperature of one of the two plasma counterstreams, the filamentation instability is diminished, i.e. for the same values of the streaming velocity, v_0, the values obtained for the growth rates in Fig. 3(b) are markedly lower than those obtained for two cold counterstreaming plasmas in Fig. 2(b).

3.1.3. Counterstreaming plasmas with finite temperature. For two symmetric counterstreams with Maxwellian distributions, shown in Fig. 4(a) and described by

$$f_0(v_x, v_y, v_z) = \frac{1}{2\pi^{3/2} v_{\rm th}^3} \times \exp\left(-\frac{v_x^2 + v_z^2}{v_{\rm th}^2}\right)\left[\exp\left(-\frac{(v_y + v_0)^2}{v_{\rm th}^2}\right) + \exp\left(-\left[\frac{(v_y - v_0)^2}{v_{\rm th}^2}\right]\right)\right], \qquad (13)$$

we find the dielectric constant

$$\epsilon_{yy} = 1 - \frac{\omega_{\rm pe}^2}{\omega^2}\left[1 + \frac{1}{2}\left(1 + \frac{2v_0^2}{v_{\rm th}^2}\right) Z'\left(\frac{\omega}{k v_{\rm th}}\right)\right], \qquad (14)$$

and plot its aperiodic solutions ($\omega_r = 0$) in Fig. 4(b).

https://doi.org/10.1017/S0022377807007015 Published online by Cambridge University Press

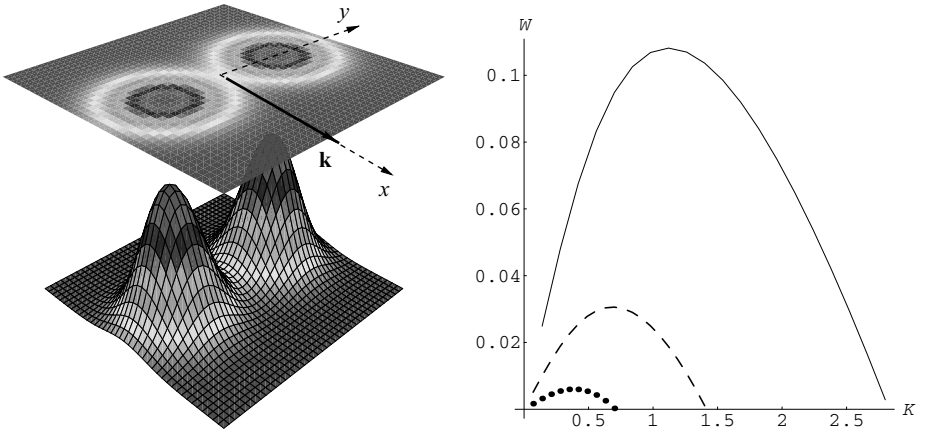

(a) (b)

Figure 4. (a) Distribution function for two symmetric counterstreaming plasmas given by (13). (b) Growth rates of the filamentation instability obtained as solutions of (14), with $v_{\rm th}/c = 0.1$ and for the same values of the streaming velocity, $v_0/c = 0.05$ (dotted curve), $v_0/c = 0.1$ (dashed curve) and $v_0/c = 0.2$ (solid curve).

After a quick comparison of the growth rates in Figs 2, 3 and 4, we should remark on the tendency of stabilization: the growth rates are significantly lower if the finite temperature effects are included, but the filamentation instability cannot be totally suppressed. This observation is consistent with the results of Thode et al. [20] and Cary et al. [21].

3.2. Weibel instability

The Weibel instability is the electromagnetic unstable mode developed non-resonantly ($\Re(\omega) = 0$) in a thermally anisotropic plasma. We simply take a bi-Maxwellian distribution function with two characteristic plasma temperatures (thermal velocities) defined along two orthogonal directions, $v_{\rm th,x} = v_{\rm th,z} = v_{\rm th} < v_{\rm th,y} = v_{\rm th\perp}$,

$$f_0(v_x, v_y, v_z) = \frac{1}{\pi^{3/2} v_{\rm th}^2 v_{\rm th\perp}} \exp\left[-\left(\frac{v_x^2 + v_z^2}{v_{\rm th}^2} + \frac{v_y^2}{v_{\rm th\perp}^2}\right)\right], \tag{15}$$

and presented schematically in Fig. 5(a). The dispersion relation is obtained by substituting (15) in (7)

$$\epsilon_{yy} = 1 - \frac{\omega_{\rm pe}^2}{\omega^2}\left[1 + \frac{1}{2}(A+1)Z'\left(\frac{\omega}{k v_{\rm th}}\right)\right], \tag{16}$$

and the growth rates of Weibel instability are plotted in Fig. 5(b). The thermal anisotropy is defined as $A = (v_{\rm th\perp}/v_{\rm th})^2 - 1 > 0$, and, in this case, it is assumed positive as long as $v_{\rm th\perp} > v_{\rm th}$. Weibel emission will therefore be perpendicular to the direction of higher temperature ($k_y = 0$ and we consider $\mathbf{k}$ parallel to the x-axis here) and with electric field along the same direction ($E = E_y$).

https://doi.org/10.1017/S0022377807007015 Published online by Cambridge University Press

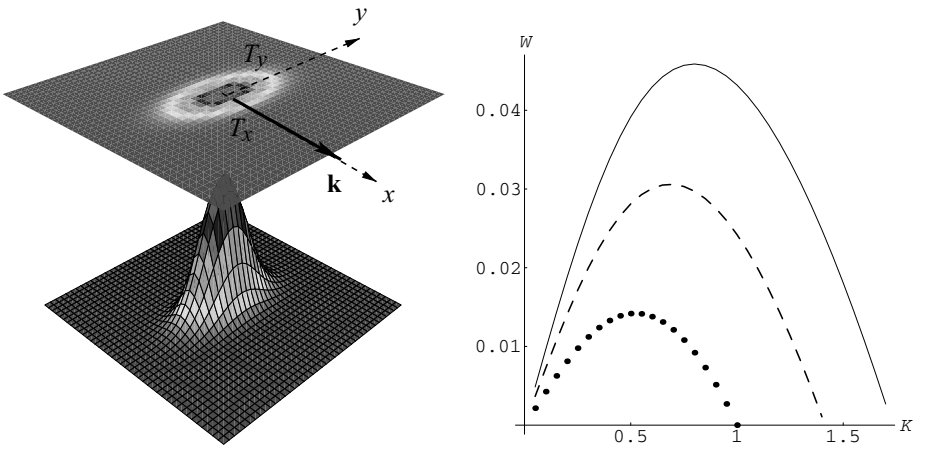

(a) (b)

Figure 5. (a) Bi-Maxwellian distribution function. (b) Growth rates of the Weibel instability obtained as solutions of (16), with $v_{\rm th}/c = 0.1$ and for the three values of the temperature anisotropy, $A = 1$ (dotted curve), $A = 2$ (dashed curve) and $A = 3$ (solid curve).

4. Cumulative effect of Weibel and filamentation instabilities: non-relativistic theory

In [24], we have already discussed two representative cases of counterstreaming plasmas with thermal anisotropies, showing that these two instabilities of filamentation and Weibel type can interact to yield larger or lower growth rates. Here, we extend our investigation to other different configurations of counterstreaming plasmas with symmetric or asymmetric thermal anisotropies.

4.1. Counterstreams with symmetric anisotropy

4.1.1. Positive anisotropy. As in [24], we can invoke firstly a symmetric configuration with two counterstreams of thermal plasmas with bi-Maxwellian distributions of equal anisotropies ($A_1 = A_2 = (v_{\rm th\perp}/v_{\rm th})^2 - 1$)

$$f_0(v_x, v_y, v_z) = \frac{1}{2\pi^{3/2} v_{\rm th}^2 v_{\rm th\perp}} \times \exp\left(-\frac{v_x^2 + v_z^2}{v_{\rm th}^2}\right)\left[\exp\left(-\frac{(v_y + v_0)^2}{v_{\rm th\perp}^2}\right) + \exp\left(-\frac{(v_y - v_0)^2}{v_{\rm th\perp}^2}\right)\right], \tag{17}$$

and which are presented schematically in Fig. 6(a). The unstable mode will be the solution of the dispersion relation

$$\epsilon_{yy} = 1 - \frac{\omega_{\rm pe}^2}{\omega^2}\left\{1 + \left[\frac{1}{2}(A+1) + \frac{v_0^2}{v_{\rm th}^2}\right] Z'\left(\frac{\omega}{k v_{\rm th}}\right)\right\}, \tag{18}$$

and cumulates now the both effects of filamentation and Weibel instabilities as is shown for three sets of parameters in Fig. 6(b) and with solid curves in Fig. 7(a) and (b).

https://doi.org/10.1017/S0022377807007015 Published online by Cambridge University Press

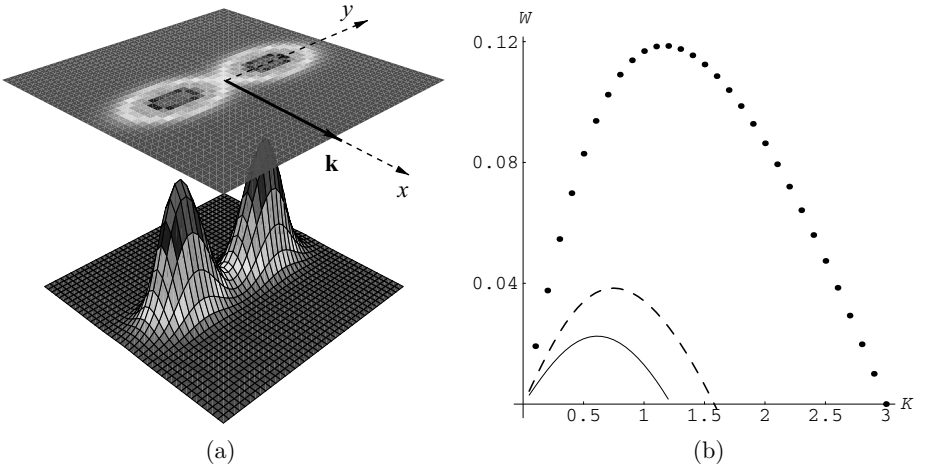

Figure 6. (a) Distribution function for two symmetric counterstreams of thermally anisotropic plasmas, given by (17). (b) Growth rates of the unstable mode, which cumulates the both effects of filamentation and Weibel instabilities, and it is solution of dispersion relation (18): for $A = 1$ and $\beta_0 = v_0/c = 0.2$ it is plotted with a dotted curve, for $A = 2$ and $\beta_0 = 0.05$ with a dashed curve, and for $A = 1$ and $\beta_0 = 0.05$ with a solid curve; $v_{\rm th}/c = 0.1$.

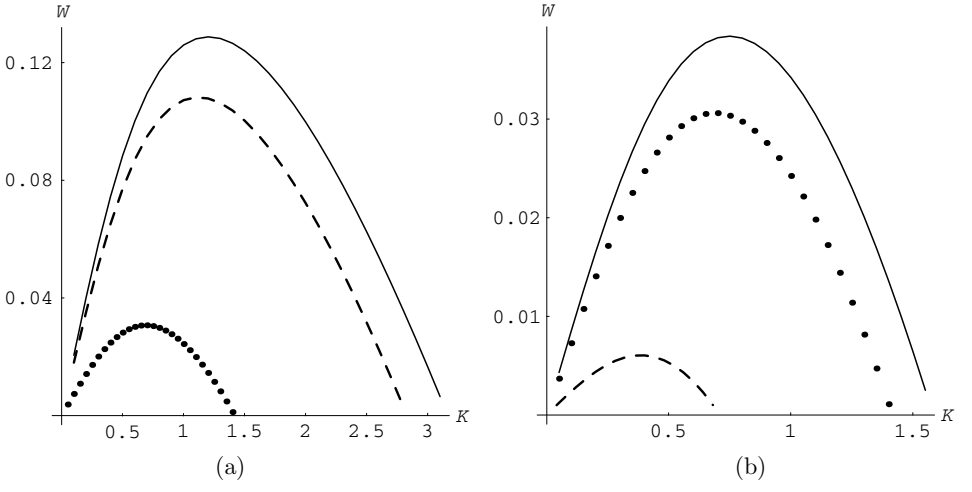

Figure 7. Comparison of the growth rates of Weibel instability (dotted curves), filamentation instability (dashed curves) and their cumulative effect (solid curves), considering $v_{\rm th}/c = 0.1$, $A = 2$ and two streaming velocities: (a) $v_0/c = 0.2$ and (b) $v_0/c = 0.05$.

Again, we compare with Fig. 2 and observe that the growth rates are significantly lower if the finite temperature effects are included, but the instability cannot be completely suppressed as predicted in [20, 21].

4.1.2. Negative anisotropy: stabilization of filamentation instability. The same distribution function (17) is considered here, but with a negative anisotropy, $A = (v_{\rm th\perp}/v_{\rm th})^2 - 1 < 0$, i.e. $v_{\rm th\perp} < v_{\rm th}$, as shown Fig. 8(a). We have already noted in [24] that the unstable emission along the x-axis (see in Fig. 1) can be diminished if the

https://doi.org/10.1017/S0022377807007015 Published online by Cambridge University Press

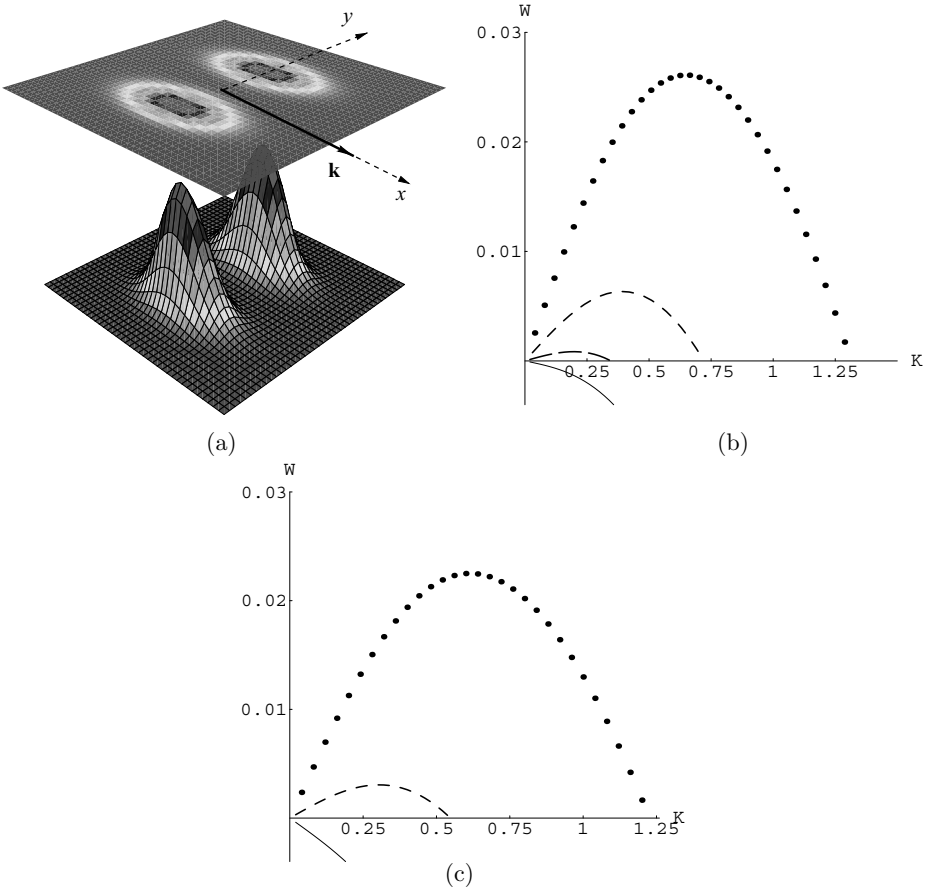

Figure 8. (a) Two counterstreaming plasmas with negative thermall anisotropies, $A < 0$ in (17); (b) The unstable modes are solutions of dispersion relation (18) and are plotted for $v_{\rm th}/c = 0.1$, $\beta_0 = 0.06$ and $A = 1$ with dotted line, for $A = -0.2$ with short dashed line, for $A = -0.6$ with long dashed line. For $A = -0.8$, with solid line (damping) are plotted the damping rates for the stabilized (damped) solutions. (c) The unstable solutions are plotted for $\beta_0 = 0.04$ and $A = 1$ with dotted line, for $A = -0.2$ with dashed line, and for $A = -0.6$ with solid line (damping).

anisotropy is of opposite sign (negative). The growth rates are provided by the same dispersion relation (18) and are plotted with dotted and dashed curves in Fig. 8(b) and (c), where we can see how are they reduced for higher (negative) anisotropies.

For a sufficiently large negative anisotropy, the cumulative effect can evenly suppress the non-resonant filamentation mode along x-axis. In this case, the only possible excitations are resonantly stabilized by collisionless damping and the imaginary solutions correspond to the damping rates and are plotted with solid curves in Fig. 8(b) and (c). This is the case of a pure Weibel regime corresponding to a Weibel emission along the y-axis (see Fig. 1).

Stabilization of the filamentation mode has been also investigated in the same manner, but for a beam–plasma system and using either simple waterbag or Maxwellian distributions; see, for example, [10] and [11], respectively. In [10] the effects of both transverse and parallel temperatures on the linear stability of

https://doi.org/10.1017/S0022377807007015 Published online by Cambridge University Press

collective electromagnetic modes, and for arbitrary wave-vector orientations ranging from two-stream longitudinal instability to filamentation transverse modes are discussed. In [11], the temperature effects were minimized assuming only the anisotropy of the background plasma. For comparison, two similar cases are also treated here in the following two sections.

4.2. Counterstreams with asymmetric anisotropy

4.2.1. Thermal counterstreaming plasmas with antisymmetric anisotropy. If the counterstreaming plasmas behave as opposite sign anisotropies, $A_1 = (v_{\mathrm{th}1\perp}/v_{\mathrm{th}})^2 - 1 > 0$, $A_2 = (v_{\mathrm{th}2\perp}/v_{\mathrm{th}})^2 - 1 < 0$, they can be modeled using the following distribution function

$$f_0(v_x, v_y, v_z) = \frac{1}{2\pi^{3/2} v_{\mathrm{th}}^2 v_{\mathrm{th}\perp}} e^{-\frac{v_x^2 + v_z^2}{v_{\mathrm{th}}^2}} \left[\frac{1}{v_{\mathrm{th}1\perp}} e^{-\frac{(v_y + v_o)^2}{v_{\mathrm{th}1\perp}^2}} + \frac{1}{v_{\mathrm{th}2\perp}} e^{-\frac{(v_y - v_0)^2}{v_{\mathrm{th}2\perp}^2}} \right], \quad (19)$$

which is schematically presented in Fig. 9(a), and substituting in (7) leads to

$$\epsilon_{yy} = 1 - \frac{\omega_{\mathrm{pe}}^2}{\omega^2} \left\{ 1 + \left[\frac{1}{4}(A_1 + A_2) + \frac{1}{2} + \frac{v_0^2}{v_{\mathrm{th}}^2} \right] Z'\left(\frac{\omega}{k v_{\mathrm{th}}} \right) \right\}. \quad (20)$$

The aperiodic solutions are shown in Fig. 9(b) and (c). For anisotropies of equal magnitudes, $A_1 = -A_2$, dispersion relation (20) reduces to

$$\epsilon_{yy} = 1 - \frac{\omega_{\mathrm{pe}}^2}{\omega^2} \left\{ 1 + \left(\frac{1}{2} + \frac{v_0^2}{v_{\mathrm{th}}^2} \right) Z'\left(\frac{\omega}{k v_{\mathrm{th}}} \right) \right\}, \quad (21)$$

which looks similarly to (14), but provides two times larger growth rates, as we can observe in Fig. 9(b). In Fig. 9(c) we show how Weibel and filamentation instabilities cumulate for a large positive anisotropy, $A_1 > |A_2|$, and generate larger growth rates (dotted curve), or how the filamentation mode is suppressed (dashed curve) for a sufficiently large negative anisotropy, $A_1 < |A_2|$.

4.2.2. Two counterstreams with cold and thermally anisotropic distributions. One of the counterstreaming plasmas is considered to be cold and the other has a thermally anisotropic particle distribution of a bi-Maxwellian type

$$f_0(v_x, v_y, v_z) = \frac{1}{2\pi^{3/2} v_{\mathrm{th}}^2 v_{\mathrm{th}\perp}} \times \exp\left(-\frac{v_x^2 + v_z^2}{v_{\mathrm{th}}^2} \right) \exp\left(-\frac{(v_y + v_0)^2}{v_{\mathrm{th}\perp}^2} \right) + \frac{1}{2} \delta(v_x) \delta(v_y - v_0) \delta(v_z), \quad (22)$$

and with (22) in (7) we find

$$\epsilon_{yy} = 1 - \frac{\omega_{\mathrm{pe}}^2}{2\omega^2} \left(1 + \frac{k^2 v_0^2}{\omega^2} \right) - \frac{\omega_{\mathrm{pe}}^2}{2\omega^2} \left\{ 1 + \left[\frac{1}{2}(A + 1) + \frac{v_0^2}{v_{\mathrm{th}}^2} \right] Z'\left(\frac{\omega}{k v_{\mathrm{th}}} \right) \right\}. \quad (23)$$

Numerical solutions of (23) are plotted in Fig. 10(b), and we observe that as long as one of the plasma streams may be considered cold, the filamentation mode cannot be stabilized by a negative and large anisotropy. Moreover, we compare with the growth rates of a pure filamentation instability in Fig. 3(b), and estimate how important the cumulative contribution of Weibel instability in Fig. 10(b) can be, as

https://doi.org/10.1017/S0022377807007015 Published online by Cambridge University Press

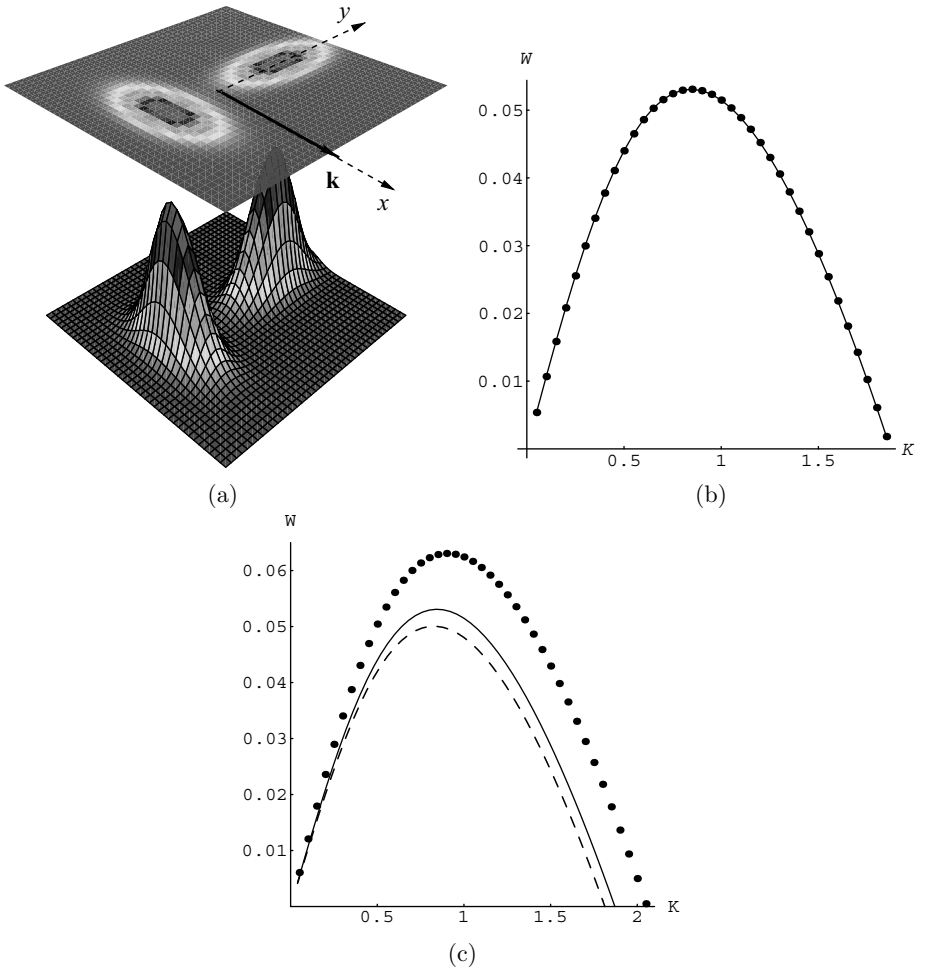

Figure 9. (a) Two counterstreaming plasmas with antisymmetric thermall anisotropies, $A_1 A_2 < 0$ in (19); (b) Growth rates of the unstable mode are the same when $A_1 = -A_2 < 1$, and they are plotted with dotted line for $v_{\rm th}/c = 0.1$, $\beta_0 = 0.2$ and $A_1 = 0.1 = -A_2$, and with solid line for $A_1 = 0.4 = -A_2$; (c) Solutions are plotted with dotted line for $A_1 = 3$, and $A_2 = -0.1$, with dashed line for $A_1 = 0.1$, and $A_2 = -0.9$, and with a solid line for $A_1 = 0.1$, and $A_2 = -0.1$.

long as the anisotropy is sufficiently large (solid and dashed curves). This case is presented only for an instructive purpose, because in the limit of a zero stationary magnetic field, plasma temperature effects must be included [21].

4.2.3. Two counterstreams with isotropic and anisotropic distributions. This final case is close to that considered by Bret and Deutsch [11]. They investigated the interplay between filamentation and Weibel instability considering a Maxwellian relativistic beam, interacting with an anisotropic plasma with a bi-Maxwellian distribution function. In order to complete our comparative study here, we assume now the same configuration but where the bulk streaming velocity, v_0, is limited to

https://doi.org/10.1017/S0022377807007015 Published online by Cambridge University Press

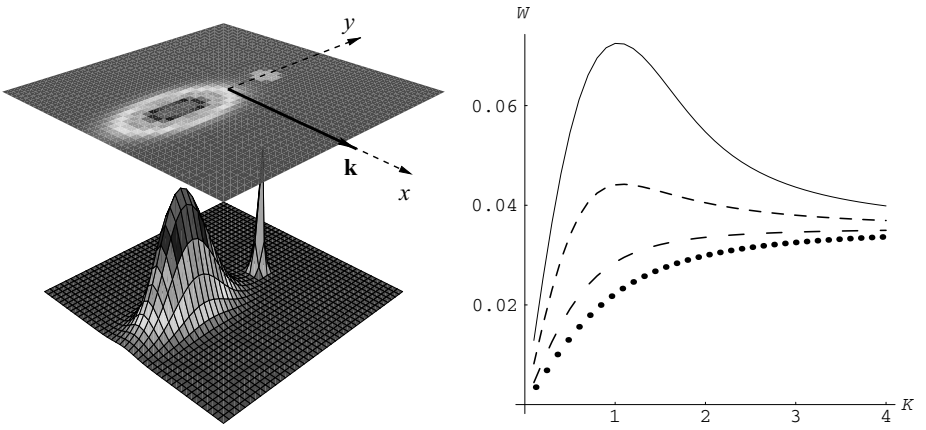

(a) (b)

Figure 10. (a) Two counterstreaming plasmas: one is assumed to be cold and the other with a temperature anisotropy of a bi-Maxwellian type. (b) Growth rates for the unstable mode, which is the solution of dispersion relation (23): $v_{\rm th}/c = 0.1$ $\beta_0 = v_0/c = 0.05$ and $A = 9$ with a solid curve, $A = 4$ with a dashed curve, $A = 0$ with a long dashed curve and $A = -3$ with a dotted curve.

non-relativistic values

$$f_0(v_x, v_y, v_z) = \frac{1}{2\pi^{3/2} v_{\rm th}^2} \exp\left(-\frac{v_x^2 + v_z^2}{v_{\rm th}^2}\right) \times \left[\frac{1}{v_{\rm th\perp}} \exp\left(-\frac{(v_y + v_0)^2}{v_{\rm th\perp}^2}\right) + \frac{1}{v_{\rm th}} \exp\left(-\frac{(v_y - v_0)^2}{v_{\rm th}^2}\right)\right] \tag{24}$$

and from (7) is obtained with the corresponding dispersion relation

$$\epsilon_{yy} = 1 - \frac{\omega_{\rm pe}^2}{\omega^2}\left\{1 + \left[\frac{1}{2}\left(1 + \frac{A}{2}\right) + \frac{v_0^2}{v_{\rm th}^2}\right] Z'\left(\frac{\omega}{k v_{\rm th}}\right)\right\}. \tag{25}$$

In this case, the cumulative effect of Weibel and filamentation instabilities is shown in Fig. 11 with dashed and solid curves, which correspond to finite values of the thermal anisotropy. Comparing the pure filamentation growth rates ($A = 0$) plotted here with a dotted curve and in Fig. 4 for three different values of streaming velocity, v_0, we simply decide that the cumulative unstable mode (dashed and solid curves in Fig. 11) is significantly faster.

5. Conclusions

We have investigated the filamentation and Weibel instabilities and their cumulative effect in counterstreaming plasmas with isotropic or anisotropic temperature distributions of a Maxwellian type. In order to facilitate a comparative investigation for these two instabilities and to highlight the relevance of their cumulative effect, we have derived the dispersion relations and we have then plotted the growth rates systematically for different configurations of counterstreaming thermal plasmas.

For a complete comparative picture, we have first shown how the growth rates look for each of these instabilities in part (see Sec. 3). Comparing the filamentation

https://doi.org/10.1017/S0022377807007015 Published online by Cambridge University Press

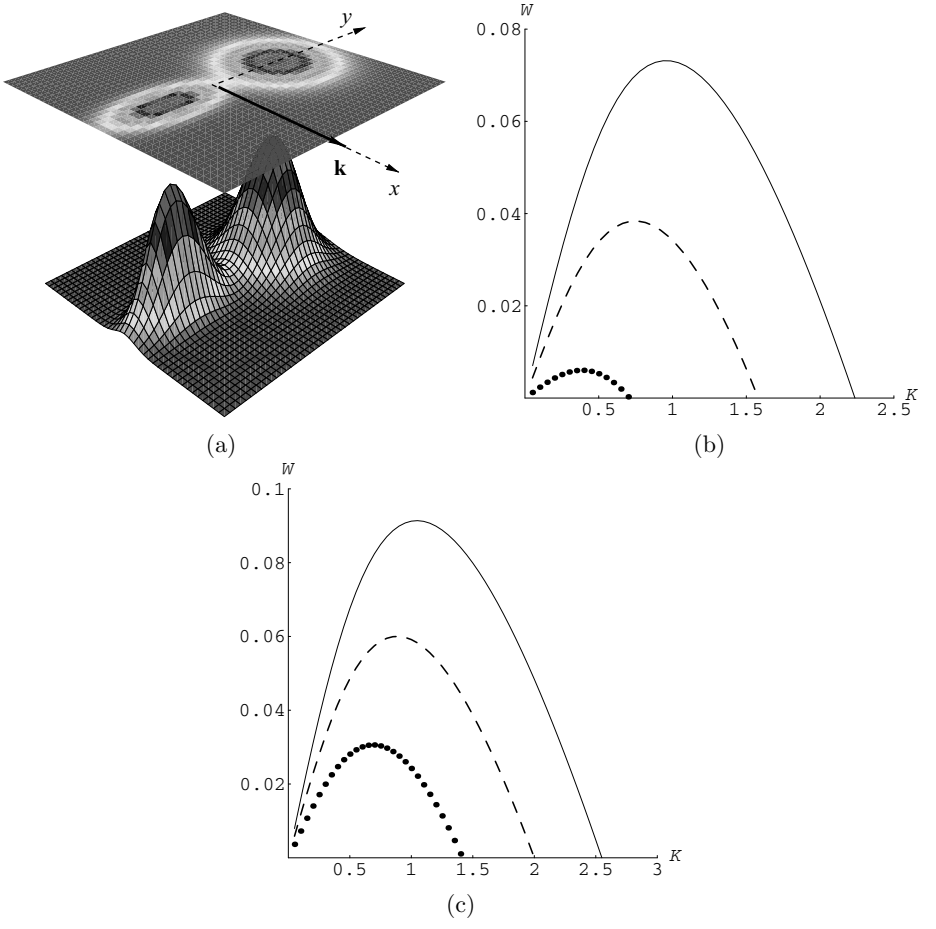

Figure 11. (a) Two counterstreaming thermal plasmas: one is assumed to isotropic and the other with a thermal anisotropy of a bi-Maxwellian type. (b) Growth rates for the unstable mode, which is a solution of dispersion relation (23): $v_{\rm th}/c = 0.1$ $\beta_0 = v_0/c = 0.05$ and $A = 9$ (solid curve), $A = 4$ (dashed curve) and $A = 0$ (dotted curve). (c) Growth rates for the unstable mode, which is solution of dispersion relation (23): $v_{\rm th}/c = 0.1$ $\beta_0 = v_0/c = 0.1$ and $A = 9$ (solid curve), $A = 4$ (dashed curve) and $A = 0$ (dotted curve).

growth rates for cold plasmas or plasmas with an isotropic Maxwellian velocity distribution function, we observe that the pure filamentation growth rates are reduced by the thermal effects.

In Sec. 4 we have extended the comparison by introducing a thermal anisotropy of a bi-Maxwellian type for each of the counterstreaming plasmas. All of the representative cases have been covered either assuming a positive or a negative temperature anisotropy, or choosing symmetric and asymmetric counterstreams.

In one of their first investigations on the stability of an unmagnetized beam–plasma system, Thode et al. [20] showed that if a finite plasma temperature is assumed, then the perpendicular temperature of the beam cannot stabilize the filamentation mode (unless there is a small amount of stationary magnetic field [21]). This can be also observed here by following successively and comparing the growth rates plotted in Secs 3.1.1, 3.1.2 and 4.2.2. In the last case, Sec. 4.2.2, it is

https://doi.org/10.1017/S0022377807007015 Published online by Cambridge University Press

suggestively shown in Fig. 10 how important the influence of the Weibel mode is as long as one of the streams behaves as a sufficiently high thermal anisotropy. We should also remark on the Weibel regime imposed by the temperature anisotropy at large wavelengths, see the solid curve in Fig. 10, where the filamentation growing mode becomes significantly faster. In this case, at saturation, the growth rate of the cumulative effect is orders of magnitude larger than that of simple filamentation mode. This contribution is diminished at small wavelengths, where the filamentation instability is not affected by the temperature anisotropy of counterstreaming plasmas. Of particular interest will in this case be the re-evaluation of the magnetic field strength reached at saturation in non-relativistic flowing models appropriate for many interstellar applications (e.g. the creation of magnetic fields in the GRBs sources of a powerful synchrotron radiation [4] or in the early universe [5]). The magnetic energy is expected to saturate to much higher values than those calculated previously considering only the simple filamentation instability of two counterstreaming cold plasmas or with isotropic Maxwellian distributions. In these new approaches should be also added the conditions under which involving baryons might enhance the magnetic energy to even higher values.

Otherwise, all beam plasma instabilities are dissipative, preventing the beam energy deposition in fusion plasma experiments, and we have shown in Sec. 4.1.2 that for a sufficiently weak ambient magnetic field and a large negative temperature anisotropy, the cumulative effect can suppress completely the non-resonant filamentation mode. Thus, it is clearly shown that kinetic effects arising from the perpendicular temperature of the beam or surrounding plasma could stabilize the non-resonant filamentation mode in fusion plasma experiments.

Relativistic flows of thermally anisotropic plasmas will be investigated in the next paper of this series. Such a new comparative analysis would be essential in getting further support for the filamentation instability (enhanced by the Weibel effect) as the most plausible mechanism for the origin of the quasistatic magnetic field in astrophysical systems containing relativistic jets, e.g., active galactic nuclei, gamma-ray bursts, galactic microquasar systems and Crab-like supernova remnants.

Acknowledgements

ML acknowledge financial support from the Alexander von Humboldt Foundation for a renewed research period in Germany. This work was supported by the NSERC Canada and by the Deutsche Forschungsgemeinschaft through the Sonderforschungsbereich 591.

References

[1] Weibel, E. S. 1959 *Phys. Rev. Lett.* **2**, 83.

[2] Fried, B. D. 1959 *Phys. Fluids* **2**, 337.

[3] Kazimura, Y., Sakai, J. I., Neubert, T. and Bulanov, S. V. 1998 *Astrophys. J.* **498**, L183.

[4] Medvedev, M. and Loeb, A. 1999 *Astrophys. J.* **526**, 697.
Gruzinov, A. 2001 *Astrophys. J. Lett.* **563**, L15.

[5] Schlickeiser, R. and Shukla, P. K. 2003 *Astrophys. J.* **599**, L57.
Okabe, N. and Hattori, M. 2003 *Astrophys. J.* **599**, 964.

[6] Nishikawa, K.-I. et al. 2003 *Astrophys. J.* **595**, 555.
Hededal, C. B., Haugbolle, T., Frederiksen, F. J. T. and Nordlund, A. 2004 *Astrophys. J.* **617**, L107.

[7] Silva, L. O., Fonseca, R. A., Tonge, J. W., Mori, W. B. and Dawson, J. M. 2002 *Phys. Plasmas* **9**, 2458.
[8] Startsvev, E. A. and Davidson, R. C. 2003 *Phys. Plasmas* **10**, 4829.
[9] Bret, A., Firpo, M.-C. and Deutsch, C. 2004 *Phys. Rev.* E **70**, 046401.
[10] Bret, A., Firpo, M.-C. and Deutsch, C. 2005 *Phys. Rev.* E **72**, 016403.
[11] Bret, A. and Deutsch, C. 2006 *Phys. Plasmas* **13**, 022110.
[12] Kalman, G., Montes, C. and Quemada, D. 1968 *Phys. Fluids* **11**, 1797.
[13] Davidson, R. C., Hammer, D. A., Haber, I. and Wagner, C. E. 1972 *Phys. Fluids* **15**, 317.
[14] Yoon, P. H. 1989 *Phys. Fluids* B **1**, 1336.
[15] Schlickeiser, R. 2004 *Phys. Plasmas* **11**, 5532.
[16] Yoon, P. H. and Davidson, R. C. 1987 *Phys. Rev.* A **35**, 2718.
[17] Yang, T.-Y. B., Gallant, Y., Arons, J. and Langdan, A. B. 1993 *Phys. Fluids* B **5**, 3369.
[18] Zaheer, S. and Murtaza, G. 2007 *Phys. Plasmas* **14**, 022108.
[19] Lee, R. and Lampe, M. 1973 *Phys. Rev. Lett.* **31**, 23.
[20] Thode, L. E., Jones, M. E., Mostrom, M. A. and Moir, D. C. 1980 *Bull. Am. Phys. Soc.* **25**, 1037.
[21] Cary, J. R., Thode, L. E., Lemons, D. S., Jones, M. E. and Mostrom, M. A. 1981 *Phys. Fluids* **24**, 1818.
[22] Shukla, P. K., Yu, M. Y. and Lakhina, G. S. 1982 *Phys. Fluids* **25**, 2344.
[23] Lee, H. and Thode, L. E. 1983 *Phys. Fluids* **26**, 2707.
[24] Lazar, M., Schlickeiser, R. and Shukla, P. K. 2006 *Phys. Plasmas* **13**, 102107.
[25] Tautz, R. C. and Schlickeiser, R. 2005 *Phys. Plasmas* **12**, 072101.
[26] Tautz, R. C. and Schlickeiser, R. 2005 *Phys. Plasmas* **12**, 122901.
[27] Tautz, R. C. and Schlickeiser, R. 2006 *Phys. Plasmas* **13**, 062901.
[28] Tautz, R. C. and Sakai, J.-I. 2007 *Phys. Plasmas* **14**, 012104.
[29] Fried, B. D. and Conte, S. D. 1961 *The Plasma Dispersion Function*. New York: Academic Press.